ACS Catalysis

Research Article

pubs.acs.org/acscatalysis

Selective Hydrogen Peroxide Formation by Titanium Dioxide Photocatalysis with Benzylic Alcohols and Molecular Oxygen in Water

Yasuhiro Shiraishi,* Shunsuke Kanazawa, Daijiro Tsukamoto, Akimitsu Shiro, Yoshitsune Sugano, and Takayuki Hirai

Research Center for Solar Energy Chemistry and Division of Chemical Engineering, Graduate School of Engineering Science, Osaka University, Toyonaka 560-8531, Japan

Supporting Information

ABSTRACT: Photocatalytic production of hydrogen peroxide (H_2O_2) on semiconductor catalysts with alcohol as a hydrogen source and molecular oxygen (O_2) as an oxygen source has attracted much attention as a potential method for safe H_2O_2 synthesis, because the reaction can be carried out without the use of explosive H_2/O_2 mixed gases. Early reported photocatalytic systems with aliphatic alcohol as a hydrogen source, however, produce only a few millimolar levels of H_2O_2. We found that benzylic alcohols, when used as a hydrogen source for photoreaction in water with titanium dioxide (TiO_2) photocatalyst, produce a very high concentration of H_2O_2 (ca. 40 mM). Raman spectroscopy and electron spin resonance analysis revealed that the enhanced H_2O_2 formation is due to the efficient formation of side-on coordinated peroxo species on the photoactivated TiO_2 surface, via the reaction of benzylic alcohol and O_2. The peroxo species is readily transformed to H_2O_2, thus facilitating highly efficient H_2O_2 production.

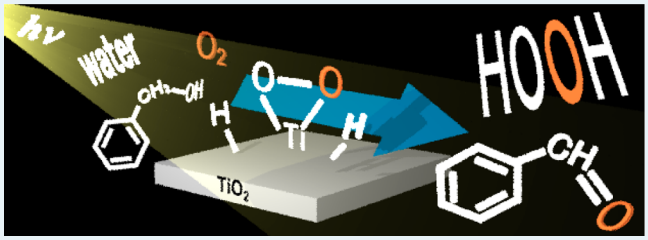

KEYWORDS: *photocatalysis, hydrogen peroxide, titanium dioxide, peroxide, surface chemistry*

INTRODUCTION

Hydrogen peroxide (H_2O_2) is a clean oxidant that emits only water as a byproduct and is widely used in industry for organic synthesis, pulp bleaching, wastewater treatment, and disinfection.[1] H_2O_2 is commercially produced by the anthraquinone method, which has some nongreen features such as high energy utilization because of the multistep hydrogenation and oxidation reactions. Recently, H_2O_2 production with H_2 and O_2 gases has been studied extensively with Pd[2−4] or Au−Pd bimetallic nanoparticle catalysts.[5−7] This direct synthesis is potentially an alternative process for H_2O_2 production from the viewpoint of green and sustainable chemistry, but some care is necessary for its operation because of the potentially explosive nature of H_2/O_2 gas mixtures.

Photocatalytic production of H_2O_2 with semiconductor titanium dioxide (TiO_2) has also attracted much attention.[8−11] The reaction is usually carried out by UV irradiation of TiO_2 suspended in an O_2-saturated water with alcohol as electron and proton donor. Photoexcitation of TiO_2 produces electron (e^-) and positive hole (h^+) pairs. The h^+ oxidizes alcohol and produces aldehyde and protons.

$$R{-}CH_2OH + 2h^+ \rightarrow R{-}CHO + 2H^+ \quad (1)$$

The e^- on the TiO_2 surface (surface Ti^{3+} site) reduces O_2 and produces a superoxo radical.[12]

$$Ti^{3+}(e^-) + O_2 \rightarrow Ti^{4+}{-}O{-}O^{\bullet} \quad (2)$$

The superoxo radical is transformed to a hydroperoxo species via further reduction with e^-. Protonation of the species produces H_2O_2.[13,14]

$$Ti^{3+}(e^-){-}O{-}O^{\bullet} + H^+ \rightarrow Ti^{4+}{-}O{-}OH \quad (3)$$

$$Ti^{4+}{-}O{-}OH + H^+ \rightarrow Ti^{4+} + H_2O_2 \quad (4)$$

These reactions proceed at atmospheric pressure and room temperature without H_2 gas and can be a clean and safe H_2O_2 synthesis. The amount of H_2O_2 produced, however, is very low (<0.2 mM).[8−11] Several kinds of TiO_2 catalysts modified with fluoride,[15] or loaded with Au[16] or Au−Ag alloy nanoparticles[17] have been proposed so far; however, all of these systems still produce only a few millimolar levels of H_2O_2. The low efficiency for H_2O_2 production on the photoactivated TiO_2 surface is because the hydroperoxo species is very unstable and is easily decomposed by further reduction with e^- to inactive hydroxide anion.[12]

$$Ti^{3+}(e^-){-}O{-}OH + H^+ \rightarrow Ti^{4+} -^{\bullet} OH + OH^- \quad (5)$$

$$Ti^{3+}(e^-) -^{\bullet} OH \rightarrow Ti^{4+} + OH^- \quad (6)$$

Received: July 5, 2013
Revised: August 20, 2013
Published: August 23, 2013

   dx.doi.org/10.1021/cs400511q | ACS Catal. 2013, 3, 2222−2227

Table 1. Results for Photocatalytic H_2O_2 Production on TiO_2 under Various Conditions[a]

entry	alcohol	solvent	alcohol consumed/μmol[b]	aldehyde or ketone/μmol[b]	H_2O_2/mM[c]	H_2O_2 selectivity/%[d]
1	ethanol	water	358.0	154.6	0.3	0.4
2	1-propanol	water	340.4	204.9	0.4	0.7
3	1-hexanol	water	453.4	123.5	0.3	0.3
4	2-phenylethanol	water	771.4	257.2	8.4	5.4
5	benzyl alcohol	water	604.1	198.1	39.6	32.8
6	*p*-nitrobenzyl alcohol	water	587.9	518.5	33.1	28.2
7	1-phenylethanol	water	628.8	397.4	40.2	32.0
8[e]	benzyl alcohol	water	85.5	53.0	4.3	25.1
9[f]	benzaldehyde	water	1311.2[g]		8.6	
10	benzyl alcohol	CH_3CN/water (3/7 v/v)	483.6	278.3	26.1	27.0
11	benzyl alcohol	CH_3CN/water (7/3 v/v)	562.1	305.6	26.7	23.8
12	benzyl alcohol	CH_3CN	1284.8	673.6	21.1	8.2
13	benzyl alcohol	DMF	420.1	123.3	1.6	1.9
14	benzyl alcohol	benzotrifluoride (BTF)	1163.5	554.9	1.8	0.8

[a]Reaction conditions: solvent (5 mL), alcohol (350 mM), catalyst (50 mg), O_2 (1 atm), λ >280 nm (light intensity at 280−400 nm, 13.8 mW cm^{-2}), photoirradiation time (12 h). [b]Determined by GC. [c]Determined by redox titration with $KMnO_4$ (detection limit: 0.05 mM). [d]= [H_2O_2 formed (μmol)]/[alcohol consumed (μmol)] × 100. [e]Photoreaction was carried out under irradiation of visible light (λ >420 nm). [f]Benzaldehyde (350 mM) was used as a starting material in place of alcohol. [g]The amount of benzaldehyde consumed.

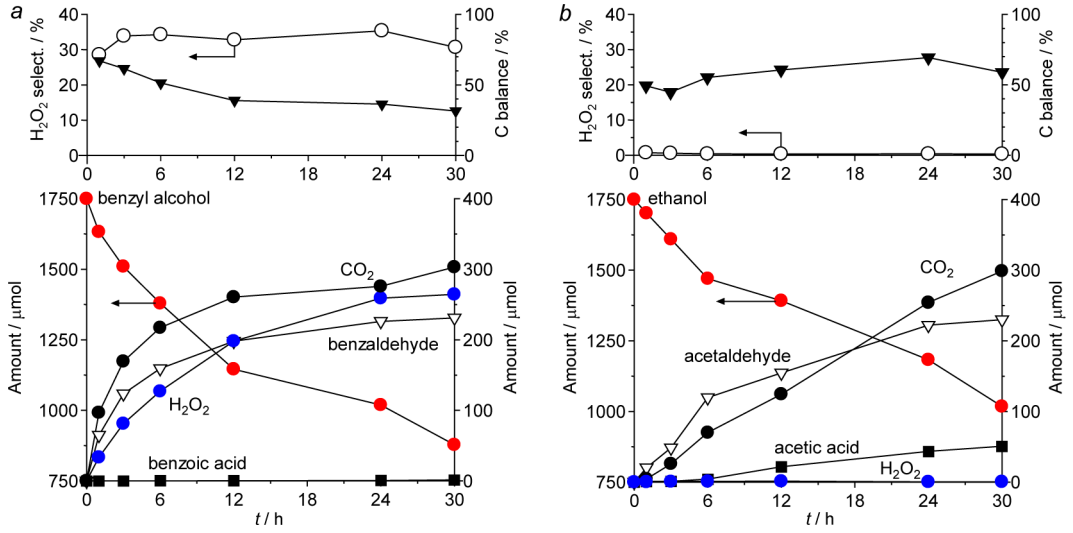

Figure 1. Time-dependent change in (bottom) the amounts of substrates and products and (top) H_2O_2 selectivity and carbon balance, during photoirradiation of TiO_2 in water with O_2 and (a) benzyl alcohol or (b) ethanol. Reaction conditions are identical to those in Table 1. The carbon balance for (a) was calculated using the equation C balance (%) = [benzaldehyde + benzoic acid + $(CO_2)/7$]/[benzyl alcohol consumed] × 100. The carbon balance for (b) was calculated using the equation, C balance (%) = [acetaldehyde + acetic acid + $(CO_2)/2$]/[ethanol consumed] × 100.

A new approach is therefore necessary for the efficient production of H_2O_2 by photocatalysis.

All of the early reported systems for photocatalytic H_2O_2 production have employed aliphatic alcohols (e.g., ethanol) as the electron and proton donor.[8−11,15−17] Herein, we report that benzylic alcohols, when used for photoreaction in water with TiO_2 and O_2, efficiently promote H_2O_2 formation. This photocatalytic system produces a very high concentration of H_2O_2 (ca. 40 mM), which is the highest concentration among the early reported systems.[8−11,15−17] Raman spectroscopy and electron spin resonance (ESR) analysis revealed that the enhanced H_2O_2 formation is because photoexcitation of TiO_2 in water with benzylic alcohols and O_2 selectively produces *side-on coordinated peroxo species* on the TiO_2 surface. This peroxo species is readily transformed to H_2O_2, resulting in efficient H_2O_2 production.

RESULTS AND DISCUSSION

Photocatalytic Activity for H_2O_2 Production. Photocatalytic reactions were carried out as follows: water (5 mL) containing TiO_2 (50 mg) and each respective alcohol (350 mM) was photoirradiated with magnetic stirring by a high-pressure Hg lamp (λ >280 nm) with O_2 (1 atm) at 298 K. Anatase TiO_2 (JRC-TIO-1; BET surface area, 73 m^2 g^{-1}; average particle size, 21 nm), kindly supplied from Catalyst Society of Japan, was used as a catalyst. Table 1 summarizes the results obtained by 12 h photoreaction. With ethanol (entry 1), the H_2O_2 concentration is 0.3 mM and the selectivity for H_2O_2 formation relative to the amount of alcohol consumed (= [H_2O_2 formed]/[alcohol consumed] × 100) is only 0.4%. Other aliphatic alcohols are also ineffective for H_2O_2 formation (entries 2−4). In contrast, as shown by entry 5, photoreaction with benzyl alcohol exhibits very high H_2O_2 selectivity (33%) and produces significantly high concentration of H_2O_2 (40

dx.doi.org/10.1021/cs400511q | ACS Catal. 2013, 3, 2222−2227

Scheme 1. Proposed Mechanism for Photocatalytic Oxidation of Alcohols with O_2 on the TiO_2 Surface

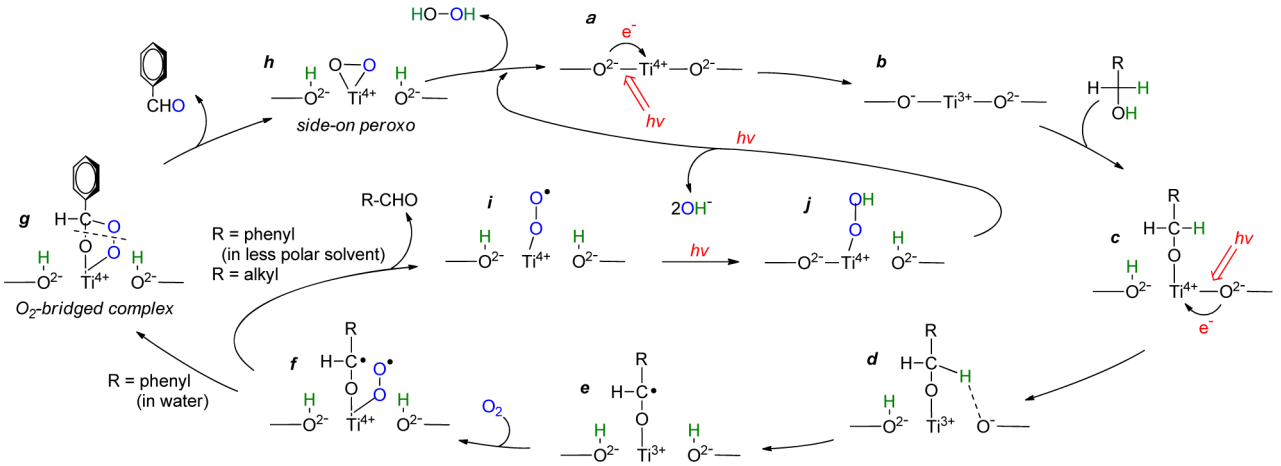

mM), which is the highest value among the photocatalytic systems reported earlier.[8−11,15−17]

Figure 1 shows the time-dependent change in the amounts of substrate and products during photoirradiation of TiO_2 with alcohol and O_2 in water. In the case with benzyl alcohol (Figure 1a), the selectivity for H_2O_2 formation is almost unchanged (>30%) even after prolonged photoirradiation (~30 h), although the rate of H_2O_2 formation decreases with photoirradiation time because of the subsequent decomposition of H_2O_2 by UV irradiation.[18] In contrast, as shown in Figure 1b, photoreaction with ethanol always shows much lower H_2O_2 selectivity (≤0.7%). As shown by entries 6 and 7 (Table 1), substituted benzylic alcohols are also effective for H_2O_2 production. In addition, the apparent quantum yield for H_2O_2 formation during photoreaction with benzyl alcohol (Φ_{AQY} (%) = [H_2O_2 formed ×2]/[photon number entering into the reaction vessel] × 100), determined with a 334 nm monochromatic light as a light source, is 29.1%, whereas the Φ_{AQY} obtained during photoreaction with ethanol is only 0.5%. These findings clearly suggest that benzylic alcohols are indeed effective for efficient and selective H_2O_2 production.

As reported,[19] benzylic alcohols are strongly adsorbed onto the TiO_2 surface, and visible light excitation of the formed charge-transferred complex promotes oxidation of alcohols. However, as shown in Table 1 (entry 8), reaction with benzyl alcohol and O_2 on TiO_2 under visible light irradiation (>420 nm) produces very small amount of H_2O_2, and the selectivity for H_2O_2 formation (25%) is lower than that obtained under UV irradiation (33%, entry 5). This suggests that band gap photoexcitation of TiO_2 promotes efficient and selective formation of H_2O_2.

It is also noted that anatase TiO_2 is effective for this reaction, as is observed for common photocatalytic reactions.[20] As shown in Supporting Information, Table S1, rutile or Degussa P25 TiO_2 [a mixture of anatase/rutile particles (ca. 80/20 wt/wt)],[21,22] produce a lower amount of H_2O_2 than anatase, although the H_2O_2 selectivities are similar.

As shown in Figure 1a, the photocatalytic reaction with benzyl alcohol produces benzaldehyde. This is decomposed by subsequent photocatalytic reaction and is finally converted to CO_2 (mineralization).[23] GC analysis of the solution detected only a small amount of benzoic acid. The carbon balance for the identified products (benzaldehyde, benzoic acid, and CO_2) is less than 50%, indicating that nonvolatile or thermally degradable ring-opening products are involved as unidentified byproducts. As shown in Table 1 (entry 9), benzaldehyde, when used as a starting material for photoreaction with TiO_2 and O_2 for 12 h, produces H_2O_2 (8.6 mM), which is much lower than that obtained with benzyl alcohol (40 mM; entry 5). This clearly suggests that photocatalytic oxidation of benzaldehyde or its photoproducts is ineffective for H_2O_2 formation; H_2O_2 is efficiently produced during photocatalytic oxidation of benzyl alcohol to benzaldehyde.

Mechanism for Enhanced H_2O_2 Production. Photocatalytic oxidation of alcohols with O_2 on TiO_2 occurs as shown in Scheme 1. Photoexcited TiO_2 (a) transfers e^- of lattice oxygen to adjacent Ti^{4+}, creating a charge-separated state (b). The e^--h^+ pairs remove the α-hydrogen of alcohol[24] and produce an alcoholate species (c). Subsequent photoexcitation removes the β-hydrogen of the species[24] (d), producing a carbon radical (e). The e^- on the Ti^{3+} site reduces O_2 and produces a superoxo radical (f).[12] In the case with benzylic alcohol, the superoxo radical combines with the adjacent carbon radical and produces a O_2-bridged complex (g). Heterolytic cleavage of the complex[25] produces the aldehyde with the exchanged O atom and side-on coordinated peroxo species (h).[26] Protonation of the side-on peroxo species produces H_2O_2 and completes the photocatalytic cycle. In contrast, with aliphatic alcohol, the combination of carbon radical and superoxo radical does not occur efficiently (f), and the aldehyde is released without exchange of O atom (i).[13] The superoxo radical left on the TiO_2 surface (i) is transformed to a hydroperoxo species (j) by further reduction with e^- (eq 3). This is decomposed to OH^- by further reduction with e^- (eqs 5 and 6). The above mechanisms indicate that photoexcitation of TiO_2 with benzylic alcohol and O_2 specifically produces side-on peroxo species (h), via the heterolytic cleavage of the O_2-bridged complex (g). This peroxo species facilitates efficient and selective H_2O_2 production.

The formation of side-on peroxo species (h) during reaction with benzylic alcohol is confirmed by Raman spectroscopy. The TiO_2 particles recovered after photoreaction (12 h) with alcohol and O_2 were used for analysis. Figure 2a shows the Raman spectrum of the TiO_2 particles recovered after photoreaction with benzyl alcohol and O_2 in water. Deconvolution of the spectrum exhibits three bands at 797, 830, and 894 cm^{-1}. The 797 cm^{-1} band is assigned to a first overtone of B_{1g} (397 cm^{-1}) mode of anatase TiO_2.[27] The 830

dx.doi.org/10.1021/cs400511q | ACS Catal. 2013, 3, 2222−2227

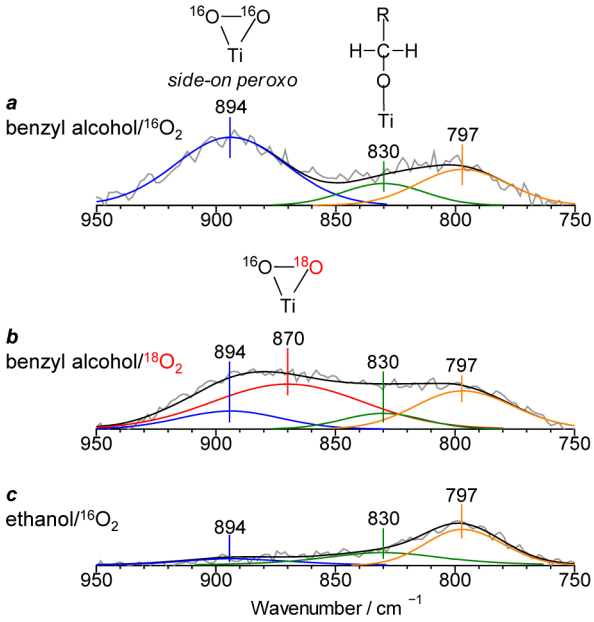

Figure 2. Raman spectra of the TiO_2 recovered after photoreaction in water with benzyl alcohol and (a) $^{16}O_2$ or (b) $^{18}O_2$, and the TiO_2 (c) recovered after photoreaction in water with ethanol and $^{16}O_2$. The reaction conditions are identical to those in Table 1.

cm^{-1} band is assigned to the C−O stretching vibration of the alcoholate species adsorbed on the TiO_2 surface (Scheme 1c).[25] The 894 cm^{-1} band is assigned to the $^{16}O-^{16}O$ stretching vibration of the side-on peroxo species on the TiO_2 surface,[25] produced by heterolytic cleavage of the O_2-bridged complex (Scheme 1g → h). The heterolytic cleavage is confirmed by the spectrum of the TiO_2 recovered after photoreaction with benzyl alcohol and labeled molecular oxygen ($^{18}O_2$) in water. As shown in Figure 2b, a new band is observed at 870 cm^{-1}, which is assigned to the $^{16}O-^{18}O$ stretching vibration. The isotopic shift (Δ = 24 cm^{-1}) is close to the shift (25 cm^{-1}) calculated based on Hooke's law for a diatomic O−O stretching.[28] These data clearly suggest that, as shown in Scheme 1, photoreaction with benzylic alcohol produces a O_2-bridged complex (g) and its heterolytic cleavage creates side-on peroxo species (h).[25] It is noted that, as shown in Figure 2b, photoreaction of benzyl alcohol with $^{18}O_2$ shows a weak signal at 894 cm^{-1} assigned to the $^{16}O-^{16}O$ side-on peroxide species. This is probably because the $^{16}O-^{18}O$ side-on peroxide species formed on the photoactivated TiO_2 surface undergo O-exchange with the $H_2{}^{16}O$ molecules, as observed for related water systems.[29]

In contrast, as shown in Figure 2c, the TiO_2 particles recovered after photoreaction with ethanol and O_2 in water scarcely exhibit an $^{16}O-^{16}O$ band. This suggests that photoreaction with ethanol scarcely produces side-on peroxo species, and the result is consistent with the very low efficiency for H_2O_2 production with ethanol (Table 1, entry 1). The above Raman spectroscopy data suggest that the formation of side-on peroxo species (Scheme 1h) is crucial for efficient H_2O_2 formation. The formation of a large number of side-on peroxo species with benzylic alcohol is explained by the stabilization of carbon radical (Scheme 1f) due to the electron delocalization on the adjacent aromatic ring.[30] This facilitates efficient coupling between the carbon radical and superoxo species (Scheme 1g), producing a large number of side-on peroxo species.

The stabilization of the carbon radical for benzylic alcohol depends strongly on the solvent polarity; highly polarized water is necessary for the efficient formation of the O_2-bridged complex. Table 1 (entries 10−14) summarizes the results for photoreaction with benzyl alcohol in different organic solvents. All of these systems show H_2O_2 selectivity lower than that obtained in water (entry 5). Figure 3 (●) shows the

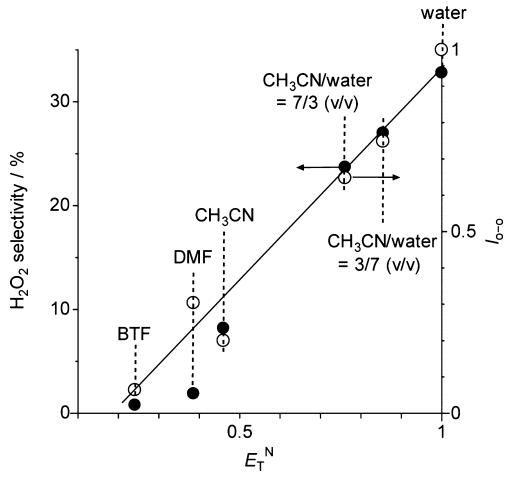

Figure 3. (●) Relationship between E_T^N of solvents and the H_2O_2 selectivity obtained by photoreaction with benzyl alcohol and O_2 (12 h) in the respective solvents (Table 1). (○) Relationship between E_T^N of solvents and the intensity (I_{O-O}) of side-on coordinated peroxo species (894 cm^{-1}) on the TiO_2 recovered after photoreaction in the respective solvents (Supporting Information, Figure S1). I_{O-O} = [{intensity of 894 cm^{-1} band in respective solvents} × {amount of benzyl alcohol consumed in water}]/[{intensity of 894 cm^{-1} band in water} × {amount of benzyl alcohol consumed in respective solvents}].

relationship between the empirical solvent polarity parameter, E_T^N,[31,32] of the solvents and the H_2O_2 selectivity obtained by photoreaction in the respective solvents (Table 1, entries 5, 10−14). A linear relationship indicates that H_2O_2 is selectively produced in more polar solvents. Figure 3 (○) shows the relationship between the E_T^N of solvents and the intensity of the $^{16}O-^{16}O$ band for side-on peroxo species (I_{O-O}) obtained by Raman analysis of TiO_2 after photoreaction with benzyl alcohol in the respective solvents (Supporting Information, Figure S1). The I_{O-O} increases with an increase in solvent polarity, and this tendency is consistent with the H_2O_2 selectivity (●). These data suggest that polar solvents indeed enhance the formation of side-on peroxo species and produce H_2O_2 more efficiently. The enhanced formation of side-on peroxo species is probably due to the stabilization of carbon radical in polar solvents[30] (Scheme 1f). This enhances the formation of the O_2-bridged complex (Scheme 1g) and creates a larger number of side-on peroxo species (Scheme 1h), resulting in enhanced H_2O_2 production in water.

The photoreaction mechanism summarized in Scheme 1 is supported by ESR analysis. Figure 4 shows the ESR spectra of the solution recovered after photoirradiation of TiO_2 with benzyl alcohol and O_2 in the presence of 5,5-dimethyl-1-pyrroline *N*-oxide (DMPO), a spin trapping reagent. With less polar CH_3CN as a solvent (Figure 4a), distinctive signals assigned to the DMPO−$O_2^{\bullet-}$ spin adduct[33] were observed (α_N = 12.7 G; α_H^β = 8.5 G; g = 2.0065). This suggests that, as shown in Scheme 1i, the superoxo radical is produced during

dx.doi.org/10.1021/cs400511q | ACS Catal. 2013, 3, 2222−2227

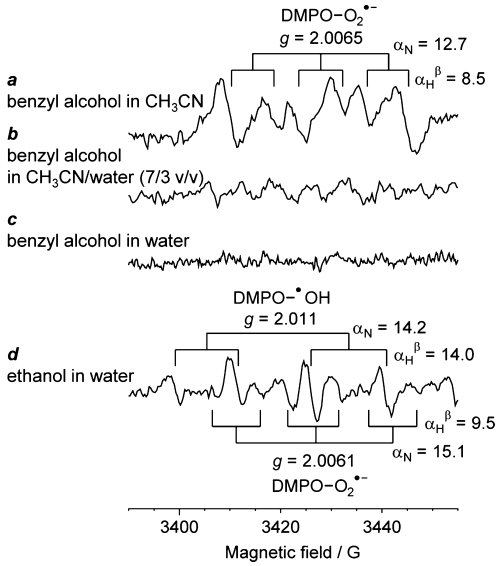

Figure 4. ESR spectra (298 K) of the DMPO spin adduct in the solutions obtained by photoirradiation of TiO_2 with benzyl alcohol and O_2 in (a) CH_3CN, (b) CH_3CN/water (7/3 v/v) mixture, and (c) water, and (d) the solution obtained by photoirradiation of TiO_2 with ethanol and O_2 in water. Reaction conditions: solvent (5 mL), TiO_2 (50 mg), alcohol (1.75 mmol), DMPO (0.1 mmol), O_2 (1 atm), photoirradiation time (15 min).

photoreaction with benzylic alcohol in less polar solvents and is trapped by the reaction with DMPO.

$$Ti^{4+}{-}O{-}O^{\bullet} + DMPO \rightarrow Ti^{4+} + DMPO{-}O_2^{\bullet -} \quad (7)$$

The intensity of the spin adduct signal decreases with an increase in the solvent polarity, and almost no signal is observed in water (Figure 4c). In contrast, as shown in Figure 3 (○), the formation of side-on peroxo species is enhanced with an increase in the solvent polarity. These data suggest that, during photoreaction with benzyl alcohol in less polar solvents (Scheme 1), the carbon radical (f) is rapidly removed and leaves the superoxo radical (i), whereas the photoreaction in polar water produces the O_2-bridged complex (g) and results in enhanced formation of side-on peroxo species (h).

Figure 4d shows the ESR spectrum of water obtained after photoreaction with ethanol and O_2. The signals for DMPO−$O_2^{\bullet -}$ spin adduct were observed (α_N = 15.1 G; α_H^{β} = 9.5 G; g = 2.0061), with signals assigned to DMPO−$^{\bullet}$OH spin adduct (α_N = 14.2 G; α_H^{β} = 14.0 G; g = 2.011),[34] which is produced by oxidation of water on the photoactivated TiO_2 ($OH^- + h^+ \rightarrow {}^{\bullet}OH$).[35] The formation of the DMPO−$O_2^{\bullet -}$ spin adduct signal suggests that, during photoreaction with aliphatic alcohol (Scheme 1), the carbon radical (f) is rapidly removed and leaves superoxo radical (i), resulting in very low efficiency for H_2O_2 formation. These data fully support the proposed mechanism (Scheme 1). Photoexcitation of TiO_2 with alcohol and O_2 produces a set of carbon radical and superoxo radical (f). In water with benzylic alcohol, the carbon radical is stabilized and transformed to the O_2-bridged complex. This produces a large number of side-on peroxo species and efficiently produces H_2O_2. In contrast, with aliphatic alcohol or with benzylic alcohol in less polar solvents, the carbon radical is unstable and is removed rapidly. This leaves the superoxo radical to be decomposed by a subsequent reaction, resulting in very low efficiency for H_2O_2 formation. These findings suggest that benzylic alcohol and water are necessary for the efficient and selective H_2O_2 formation.

CONCLUSION

We found that photoexcitation of anatase TiO_2 in water with benzylic alcohol and O_2 efficiently promotes H_2O_2 formation. This system successfully produces a very high concentration of H_2O_2 (ca. 40 mM), which is much higher than those of early reported photocatalytic systems with aliphatic alcohols. The enhanced H_2O_2 formation is due to the efficient formation of side-on peroxo species produced via the reaction of benzylic alcohols and O_2 in water. The present H_2O_2 selectivity is about 33%, and further improvement of the selectivity is necessary. Nevertheless, the concept presented here based on the selective creation of side-on coordinated peroxo species on the TiO_2 surface may contribute to the design of more efficient and selective photocatalytic systems for H_2O_2 production and may open a new strategy toward clean and safe H_2O_2 synthesis without H_2 gas.

EXPERIMENTAL SECTION

Photoreaction. TiO_2 (50 mg) was suspended in a solution (5 mL) containing each respective alcohol (1.75 mmol) within a glass tube (φ12 mm; capacity, 20 mL), and the tube was sealed with a rubber septum cap. The catalyst was dispersed well by ultrasonication for 5 min, and O_2 was bubbled through the solution for 5 min. The tube was photoirradiated at $\lambda > 280$ nm with magnetic stirring using a 450 W high pressure Hg lamp (USHIO Inc.).[17] Visible light ($\lambda > 420$ nm) irradiation was carried out with an aqueous $NaNO_2$ (20 wt %) solution as a filter.[36] The temperature of solution was kept at 298 ± 0.5 K with a digitally controlled water bath.[21] The gas-phase product was analyzed by GC-TCD (Shimadzu; GC-14B). The catalyst was recovered by centrifugation, and the liquid-phase product was analyzed by GC-FID (Shimadzu; GC2010A). The substrate and product concentrations were calibrated with authentic samples. H_2O_2 concentration was determined by the redox titration with $KMnO_4$.[23]

Quantum Yield Determination. Photoreaction was carried out using a water (2 mL) containing alcohol (0.7 mmol) and TiO_2 (20 mg) within a glass tube (φ12 mm; capacity, 20 mL). After ultrasonication and O_2 bubbling, the tube was photoirradiated with stirring using a Xe lamp (USHIO Inc.)[23] for 3 h, where the incident light was monochromated by a 334 nm band-pass glass filter (Asahi Techno Glass Co.; LX334). The full-width at half-maximum (fwhm) of the light was 9 nm. The photon number entered into the reaction vessel was determined with a spectroradiometer USR-40 (USHIO Inc.).[37]

Raman Spectroscopy. Raman spectra were measured on a confocal Raman microscope (LabRAM HR-800, HORIBA). YAG laser (532 nm line) was used as the excitation source, where the laser power was 100 mW and the total data accumulation time was 30 s. The samples were prepared as follows: After photoreaction, TiO_2 particles were recovered by centrifugation and dried at room temperature in vacuo. They were mounted on a microscope slide and subjected to analysis. The peak intensities were normalized to the peak at 797 cm^{-1} for a first overtone of B_{1g} mode for anatase TiO_2.

ESR Measurement. ESR spectra were recorded at the X-band using a Bruker EMX-10/12 spectrometer with a 100 kHz magnetic field modulation at a microwave power level of 10.5

dx.doi.org/10.1021/cs400511q | ACS Catal. 2013, 3, 2222−2227

mW, where microwave power saturation of the signals does not occur.[22] The magnetic field was calibrated using a 1,1′-diphenyl-2-picrylhydrazyl (DPPH) as standard. The measurement was carried out as follows: TiO_2 (50 mg) was suspended in a solution (5 mL) containing each respective alcohol (1.75 mmol) and DMPO (0.1 mmol) within a glass tube (φ12 mm; capacity, 20 mL), and the tube was sealed with a rubber septum cap. After ultrasonication (5 min) and O_2 bubbling (5 min), the solution was photoirradiated (λ >280 nm) for 15 min with magnetic stirring. The catalyst was recovered by centrifugation, and the resulting solution was subjected to analysis.

■ ASSOCIATED CONTENT

Supporting Information

Raman spectra of TiO_2 recovered after photoreaction with benzyl alcohol in different solvents (Figure S1), results of photocatalytic H_2O_2 production on various TiO_2 (Table S1). This material is available free of charge via the Internet at http://pubs.acs.org.

■ AUTHOR INFORMATION

Corresponding Author

*E-mail: shiraish@cheng.es.osaka-u.ac.jp.

Notes

The authors declare no competing financial interest.

■ ACKNOWLEDGMENTS

This work was supported by the Grant-in-Aid for Scientific Research (No. 23360349) from the Ministry of Education, Culture, Sports, Science and Technology, Japan (MEXT).

■ REFERENCES

(1) Campos-Martin, J. M.; Blanco-Brieva, G.; Fierro, J. L. G. *Angew. Chem., Int. Ed.* **2006**, *45*, 6962−6984.
(2) Lunsford, J. H. *J. Catal.* **2003**, *216*, 455−460.
(3) Blanco-Brieva, G.; Cano-Serrano, E.; Campos-Martin, J. M.; Fierro, J. L. G. *Chem. Commun.* **2004**, 1184−1185.
(4) Melada, S.; Rioda, R.; Menegazzo, F.; Pinna, F.; Strukul, G. *J. Catal.* **2006**, *239*, 422−430.
(5) Choudhary, V. R.; Gaikwad, A. G.; Sansare, S. D. *Angew. Chem., Int. Ed.* **2001**, *40*, 1776−1779.
(6) Landon, P.; Collier, P. J.; Papworth, A. J.; Kiely, C. J.; Hutchings, G. J. *Chem. Commun.* **2002**, 2058−2059.
(7) Edwards, J. K.; Solsona, B.; Ntainjua, E.; Carley, A. F.; Herzing, A. A.; Kiely, C. J.; Hutchings, G. J. *Science* **2009**, *323*, 1037−1041.
(8) Kormann, C.; Bahnemann, D. W.; Hoffmann, M. R. *Environ. Sci. Technol.* **1988**, *22*, 798−806.
(9) Cai, R.; Kubota, Y.; Fujishima, A. *J. Catal.* **2003**, *219*, 214−218.
(10) Goto, H.; Hanada, Y.; Ohno, T.; Matsumura, M. *J. Catal.* **2004**, *225*, 223−229.
(11) Hirakawa, T.; Nosaka, Y. *J. Phys. Chem. C* **2008**, *112*, 15818−15823.
(12) Nakamura, R.; Imanishi, A.; Murakoshi, K.; Nakato, Y. *J. Am. Chem. Soc.* **2003**, *125*, 7443−7450.
(13) Hirakawa, T.; Koga, C.; Negishi, N.; Takeuchi, K.; Matsuzawa, S. *Appl. Catal., B* **2009**, *87*, 46−55.
(14) Hirakawa, T.; Daimon, T.; Kitazawa, M.; Ohguri, N.; Koga, C.; Negishi, N.; Matsuzawa, S.; Nosaka, Y. *J. Photochem. Photobiol. A* **2007**, *190*, 58−68.
(15) Maurino, V.; Minero, C.; Mariella, G.; Pelizzetti, E. *Chem. Commun.* **2005**, 2627−2629.
(16) Teranishi, M.; Naya, S.; Tada, H. *J. Am. Chem. Soc.* **2010**, *132*, 7850−7851.
(17) Tsukamoto, D.; Shiro, A.; Shiraishi, Y.; Sugano, Y.; Ichikawa, S.; Tanaka, S.; Hirai, T. *ACS Catal.* **2012**, *2*, 599−603.
(18) Li, X.; Chen, C.; Zhao, J. *Langmuir* **2001**, *17*, 4118−4122.
(19) Higashimoto, S.; Kitao, N.; Yoshida, N.; Sakura, T.; Azuma, M.; Ohue, H.; Sakata, Y. *J. Catal.* **2009**, *266*, 279−285.
(20) Tanaka, K.; Capule, M. F. V.; Hisanaga, T. *Chem. Phys. Lett.* **1991**, *187*, 73−76.
(21) Tsukamoto, D.; Shiraishi, Y.; Sugano, Y.; Ichikawa, S.; Tanaka, S.; Hirai, T. *J. Am. Chem. Soc.* **2012**, *134*, 6309−6315.
(22) Sugano, Y.; Shiraishi, Y.; Tsukamoto, D.; Ichikawa, S.; Tanaka, S.; Hirai, T. *Angew. Chem., Int. Ed.* **2013**, *52*, 5295−5299.
(23) Tsukamoto, D.; Ikeda, M.; Shiraishi, Y.; Hara, T.; Ichikuni, N.; Tanaka, S.; Hirai, T. *Chem.—Eur. J.* **2011**, *17*, 9816−9824.
(24) Shishido, T.; Miyatake, T.; Teramura, K.; Hitomi, Y.; Yamashita, H.; Tanaka, T. *J. Phys. Chem. C* **2009**, *113*, 18713−18718.
(25) Zhang, M.; Wang, Q.; Chen, C.; Zang, L.; Ma, W.; Zhao, J. *Angew. Chem., Int. Ed.* **2009**, *48*, 6081−6084.
(26) Jeske, P.; Haselhorst, G.; Weyhermueller, T.; Wieghardt, K.; Nuber, B. *Inorg. Chem.* **1994**, *33*, 2462−2471.
(27) Tompsett, G. A.; Bowmaker, G. A.; Cooney, R. P.; Metson, J. B.; Rodgers, K. A.; Seakins, J. M. *J. Raman Spectrosc.* **1995**, *26*, 57−62.
(28) Tsilomelekis, G.; Boghosian, S. *J. Phys. Chem. C* **2011**, *115*, 2146−2154.
(29) Risley, J. M.; Van Etten, R. L. *J. Am. Chem. Soc.* **1981**, *103*, 4389−4392.
(30) Ito, O.; Matsuda, M. *J. Am. Chem. Soc.* **1982**, *104*, 568−572.
(31) Reichardt, C. *Chem. Rev.* **1994**, *94*, 2319−2358.
(32) Johnson, B. P.; Khaledi, M. G.; Dorsey, J. G. *Anal. Chem.* **1986**, *58*, 2354−2365.
(33) Wang, W.; Ng, T. W.; Ho, W. K.; Huang, J.; Liang, S.; An, T.; Li, G.; Yu, J. C.; Wong, P. K. *Appl. Catal., B* **2013**, *129*, 482−490.
(34) Lin, F.; Zhang, Y.; Wang, L.; Zhang, Y.; Wang, D.; Yang, M.; Yang, J.; Zhang, B.; Jiang, Z.; Li, C. *Appl. Catal., B* **2012**, *127*, 363−370.
(35) Hirakawa, T.; Nosaka, Y. *Langmuir* **2002**, *18*, 3247−3254.
(36) Shiraishi, Y.; Sugano, Y.; Ichikawa, S.; Hirai, T. *Catal. Sci. Technol.* **2012**, *2*, 400−405.
(37) Koizumi, H.; Shiraishi, Y.; Tojo, S.; Fujitsuka, M.; Majima, T.; Hirai, T. *J. Am. Chem. Soc.* **2006**, *128*, 8751−8753.